NASA Technical Memorandum 86436

SELECTED TOPICS IN EXPERIMENTAL AEROELASTICITY AT THE NASA LANGLEY RESEARCH CENTER

RODNEY H. RICKETTS

APRIL 1985

NASA
National Aeronautics and Space Administration

Langley Research Center
Hampton, Virginia 23665

SELECTED TOPICS IN EXPERIMENTAL AEROELASTICITY AT THE NASA LANGLEY RESEARCH CENTER

Rodney H. Ricketts*

National Aeronautics and Space Administration
Washington, D.C. 20546

ABSTRACT

The National Aeronautics and Space Administration (NASA) conducts research in aeroelasticity to develop new technologies for aerospace-vehicle applications, to study innovative configuration changes for improved flight performance, and to develop new methods of testing for aeroelastic instabilities. This paper presents the results of selected studies that have been conducted by the NASA Langley Research Center in the last three years. The topics presented focus primarily on the ever-important transonic flight regime and include the following: body-freedom flutter of a forward-swept-wing configuration with and without relaxed static stability; instabilities associated with a new tilt-rotor vehicle; effects of winglets, supercritical airfoils, and spanwise curvature on wing flutter; wind-tunnel investigation of a "flutter-like" oscillation on a high-aspect-ratio flight research wing; results of wind-tunnel demonstration of the NASA decoupler pylon concept for passive suppression of wing/store flutter; and, new flutter testing methods which include testing at cryogenic temperatures for full scale Reynolds number simulation, subcritical response techniques for predicting onset of flutter, and a two-degree-of-freedom mount system for testing side-wall-mounted models.

I. INTRODUCTION

The National Aeronautics and Space Administration (NASA) conducts research in aeroelasticity to develop new technologies for aerospace-vehicle applications, to study innovative configuration changes for improved flight performance, and to develop new methods of testing for aeroelastic response. A group of about 30 researchers at the Langley Research Center is engaged in the experimental and analytical studies to understand, predict, and control various aeroelastic phenomena. Some of the areas of work are shown in Fig. 1. These areas include studies of advanced configurations, concepts to control response, flutter clearance of prototype aircraft, and measurement and prediction of unsteady aerodynamic forces. Because the most critical flight region for aeroelasticity occurs at transonic Mach numbers, the work is focused on that speed range. The accomplishments of recent studies sponsored by the Langley Research Center and plans for future research are contained in Ref. 1-3.

This paper presents the results of some selected studies in experimental aeroelasticity conducted since the previous international aeroelasticity symposium at which the highlights[4] of two decades of studies were presented. This paper discusses the two transonic wind tunnels that were used in these studies, some new techniques used to facilitate testing, and the aeroelastic characteristics of some advanced configurations tested. Results from companion studies in unsteady aerodynamics are presented in Ref. 5 and will not be described herein.

II. FACILITIES

Most of the experimental studies in aeroelasticity performed at Langley Research Center are conducted in the Transonic Dynamics Tunnel. However, with the recent interest in high Reynolds number testing using cryogenics, some tests have been conducted in the 0.3-m Transonic Cryogenic Tunnel. These two facilities are described here.

Transonic Dynamics Tunnel

The Transonic Dynamics Tunnel (TDT) is a closed-circuit, continous-flow, single-return wind tunnel that utilizes either air or Freon-12**(dichlorodifluoromethane) as a test medium. An aerial view of the TDT and the attached engineering and equipment building is shown in Fig. 2. Characteristics and special features of the wind tunnel are listed in Table 1 and described here and in more detail in Ref. 4. The TDT test section is 4.9 m (16 ft) square with cropped corners. The Mach number ranges

*Program Manager, Material and Structures Division, Office of Aeronautics and Space Technology; on detail from Loads and Aeroelasticity Division, NASA Langley Research Center.

**Registered trademark of E.I. du Pont de Nemours & Co., Inc.

Figure 1. Some elements of NASA aeroelasticity program.

from zero to about 1.2, and the total (stagnation) pressure ranges from about zero to one atmosphere. The maximum Reynolds number obtainable is about three million per meter (nine million per foot). A computerized data acquisition system is incorporated to measure model responses and, in some cases, to control the model inputs. By-pass valves are present in the wind-tunnel circuit to decrease quickly the dynamic pressure in the test section in the event of a model instability. The tunnel fan blades are protected from debris of damaged models by a wire-mesh safety screen. In addition to typical sidewall and sting mount systems for models, a special two-cable mount system is available for "flying" full-span models. The system provides five degrees of freedom with movement in the drag direction only being restrained. Finally, gust vanes can be mounted upstream of the test section on the sidewalls and oscillated sinusoidally to provide a gust environment for the models.

The TDT currently is undergoing an upgrade that includes two major items. First, the limiting test density capability is being increased by fifty percent in the transonic region as shown in Fig. 3. This

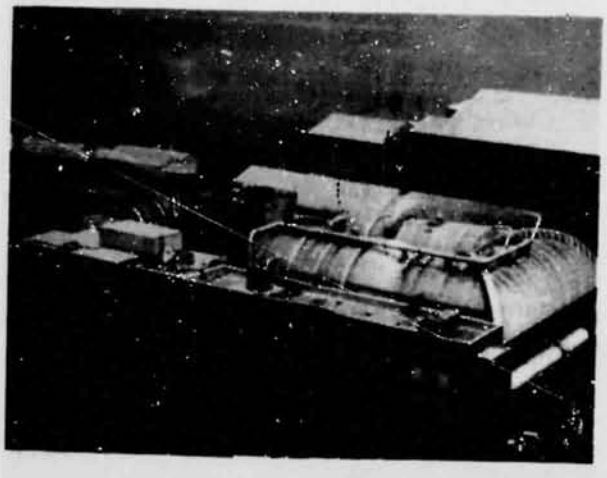

Figure 2. Transonic Dynamics Tunnel (TDT).

Tunnel characteristics

• Test section	4.9 m × 4.9 m (16' × 16')
• Mach range	0 to 1.2
• Test medium	Air or Freon-12
• Total pressure	0.01 to 1.0 atmos
• Reynolds no. (max)	3×10^6/m (10^7/ft)

Special testing features

- Computerized data acquisition system
- "0 - stopper" for flutter testing
- tunnel - fan safety screen
- suspension systems for "free-flying" models
- Gust generator

Table 1. Characteristics and features of TDT.

is being accomplished by increasing the motor power by fifty percent to 22.4 megawatts (30,000 hp). A new power distribution system and additional cooling capacity are required for this modification. Completion and checkout of this upgrade is scheduled for spring of 1985. Second, the current data acquisiton system is being replaced by a new system which will include three central processor units (CPU) to improve performance and to increase reliability by adding redundancy. The new computer system is scheduled to be fully operational in 1987.

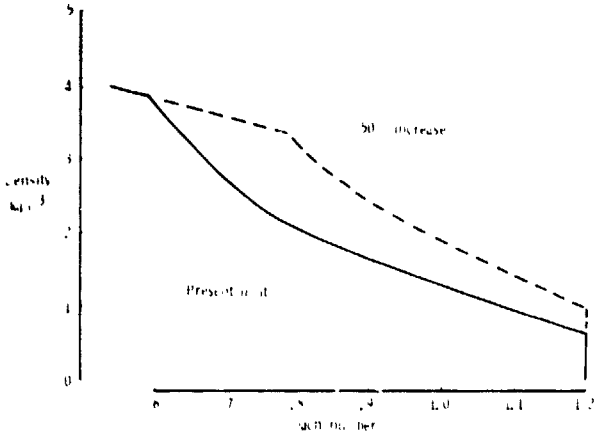

Figure 3. Increased performance of TDT.

Transonic Cryogenic Tunnel

The 0.3-m Transonic Cryogenic Tunnel[7] (TCT) is a closed-circuit continous-flow wind tunnel that provides capability for testing at high Reynolds number by a combination of low temperature and high pressure. Cryogenic temperatures are obtained by injecting liquid nitrogen (78 °K) into the tunnel circuit. The stagnation pressure can be varied from about one to six atmospheres. Mach number can be varied from zero to 0.9 in a 2-D test section which is 20 cm by 60 cm. (An interchangeable 3-D section has a Mach number capability of 1.2.) A typical tunnel operating envelope is shown in Fig. 4 for a Mach number of 0.85. This envelope indicates the range of dynamic pressure and Reynolds number available for testing. The conditions that define the boundaries are the maximums and minimums of stagnation temperature T_t and stagnaion pressure P_t. Conventional tunnels operate along or near ambient temperature lines, and increases in Reynolds number are obtained by increases in stagnation pressure. However, with the addition of temperature as a variable, Reynolds number capability is greatly increased to a maximum of about 400 million per meter (122 million per foot). Pure aeroelastic studies can be conducted along lines of constant Reynolds number. Pure Reynolds number studies can be conducted along lines of constant dynamic pressure.

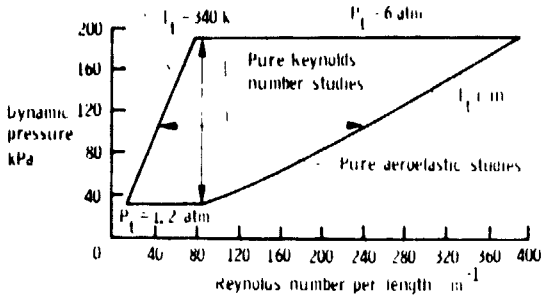

Figure 4. 0.3-m Transonic Cryogenic Tunnel operating envelope at 0.85 Mach number.

III. TESTING TECHNIQUES

To study effectively the many facets of aeroelasticity, it has been necessary to improve and expand the methods of testing. Three new or advanced techniques for flutter testing are described here.

Subcritical Response Methods

To reduce the risk of model damage during flutter testing, subcritical response (SR) methods are used to predict an impending flutter condition. Data are acquired and analyzed to determine the stability of the model at several test conditions. The results are then extrapolated to determine the test condition at which the model would be unstable. Four SR methods[8] were evaluated on a cantilevered wing model which was tested in the TDT. The wing was a 0.25-scale model representative of an advanced fighter airplane. The study included the peak-hold spectrum, cross-spectrum, power spectral density (PSD), and randomdec methods illustrated in Fig. 5.

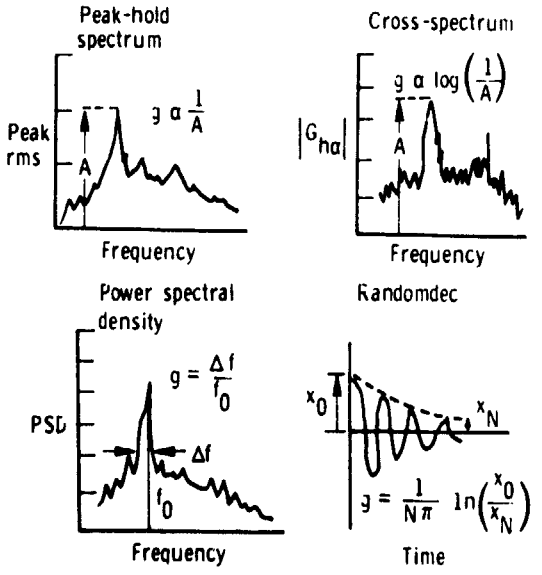

Figure 5. Four subcritical response methods for predicting flutter onset.

Each method is briefly described as follows. For the peak-hold spectrum method, damping g is proportional to the inverse of amplitude A of the peak root-mean-square (RMS) value. For the cross-spectrum method (a new method), damping is proportional to the logarithm of the inverse amplitude of the cross-spectrum value. (For example, this method measures quantitatively the coupling between bending and torsion motions that occur as flutter is approached.) For the PSD method, damping is equal to the ratio of the frequency width f at the half-power point to the nominal frequency f_o of the PSD peak. For the randomdec method, damping is equal to the logarithmic decrement of an ensemble averaged time history trace.

Model response from aerodynamic turbulence was measured using bending and torsion gages at the wing root. Results of the study are presented in Fig. 6 for data at Mach number 0.82. For this case, all four SR methods provided flutter-mode damping trends from which a flutter dynamic pressure could be predicted reliably. This is seen clearly by comparing each predicted flutter point with the actual experimental flutter point (9.00 kPa). Although there are advantages and disadvantages to each method, the peak-hold and cross-spectrum methods appear to be the best suited for on-line, near real-time use because they provide damping trends more easily and readily than the other two methods. However, to acquire actual values of damping, the PSD or randomdec methods must be used.

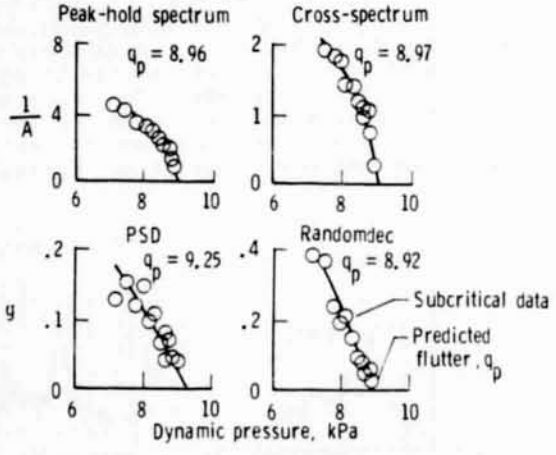

Figure 6. Results from four subcritical response methods.

New Mount System

Flutter is a complex phenomena that occurs because of the interaction of stiffness, aerodynamic and inertia forces. To understand the mechanics of flutter of new configurations, it is often necessary to separate the interacting parts. This can be done using a new sidewall model mount system[9] that is being developed for the TDT. In this system, stiffness variables

Figure 7. Pitch and plunge apparatus (PAPA).

are provided through root flexures, aerodynamic forces are isolated on a "rigid" wing model, and mass properties are obtained by using ballast weights. A prototype system, called PAPA for Pitch and Plunge Apparatus, with a wing model attached is shown in Fig. 7. The system provides flexibility in the pitch and plunge directions through an arrangement (Fig. 8) of circular rods and drag strut that attaches a splitter plate to the sidewall turntable. The model is attached to the splitter plate which acts as a reflection plane. The system mechanics require the

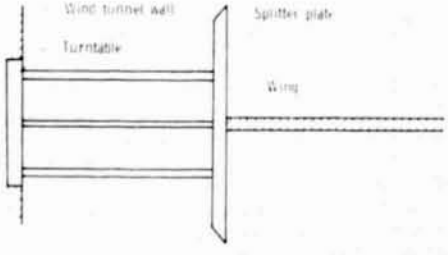

(a) Looking upstream (windscreen not shown).

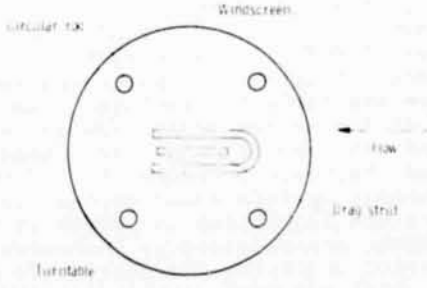

(b) Looking perpendicular to turntable face.

Figure 8. Horizontal views of PAPA componets.

splitter plate to move parallel to the side wall. Pitch stiffness (torsion) and plunge stiffness (bending) can be varied by proper choices of rod size, length and placement. The strut is provided to increase the stiffness in the drag direction. Main advantages of the PAPA include low friction damping, high strength, and low stiffness characteristics.

Some flutter results obtained using PAPA are shown in Fig. 9. The semispan model that was tested had a rectangular planform of aspect ratio three and a NACA 64A010 airfoil shape. These flutter data were acquired at subsonic Mach numbers for a large variation in angle of attack. The results show both classical flutter and stall flutter bundaries. The stall flutter occurred at approximately eight degrees and beyond. Currently, a refined mount system is being fabricated for use in the TDT. This design incorporates a large fixed splitter plate with shrouds that completely cover the rod supports.

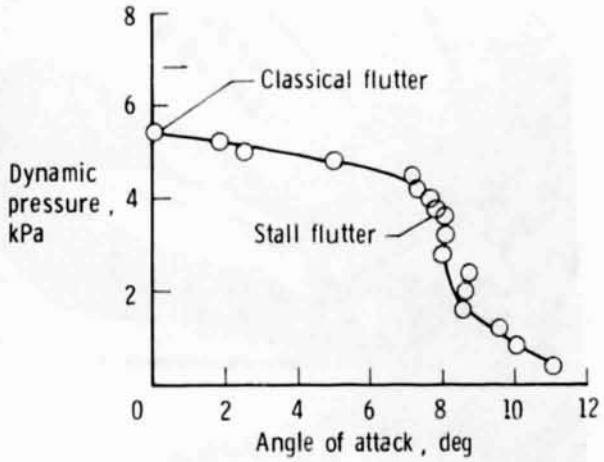

Figure 9. Flutter boundary of wing on PAPA.

Cryogenic Flutter Testing

A model wing was designed and fabricated of Vascomax† (18 Ni grade 200 maraging steel) for testing in the cryogenic wind tunnel to determine the best methods for flutter testing at cryogenic temperatures and to determine the effect of Reynolds number on flutter. The wing, shown in Fig. 10, was "rigid" and had a ten percent thick NACA 64A010 airfoil shape and a panel aspect ratio of 1.3. A beam flexure that provided bending and torsion degrees of freedom attached the wing root to a cantilever mount behind the tunnel wall. Two procedures for acquiring flutter data were investigated during the tests. These are

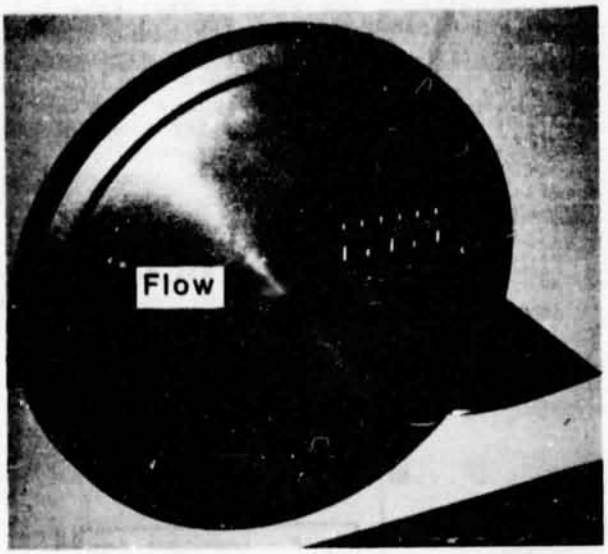

Figure 10. Model in cryogenic tunnel.

illustrated in Fig. 11 as Procedures 1 and 2. During Procedure 1, Mach number and Reynolds number were held constant by varying both stagnation temperature and pressure. This method was slow and required additional time to allow the model temperature to stabilize after each change in tunnel conditions. During Procedure 2, Mach number and stagnation temperature were held constant and only stagnation pressure was varied. Although in this case Reynolds number varied, this procedure proved to be the most effective and efficient.

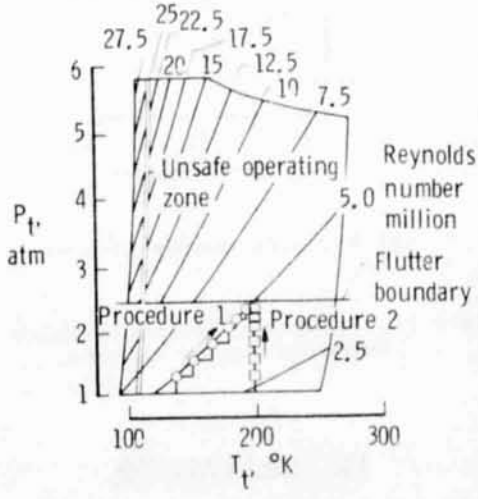

Figure 11. Two approaches to flutter boundary in TCT at 0.8 Mach number.

†Registered trademark of Teledyne Vasco.

Results of the wing flutter test are presented in Fig. 12. The flutter boundary (Fig. 12a) shows only slight differences in flutter dynamic pressures at various stagnation temperatures T_t. Analyses using kernel function aerodynamics compare favorably with the experimental results. Through additional analyses, the mass ratio effect was removed from the flutter data to isolate the Reynolds number effect (Fig. 12b). These results indicate that the flutter dynamic pressure was reduced approximately five percent by increasing the Reynolds number over the range tested.

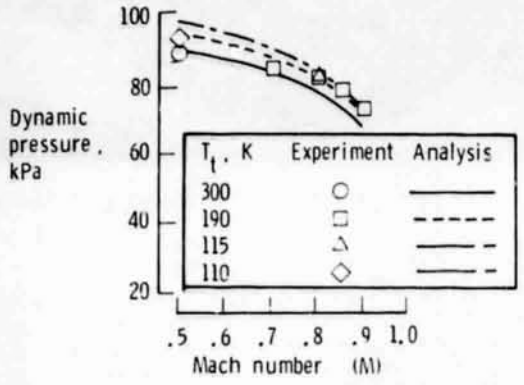

(a) Flutter results.

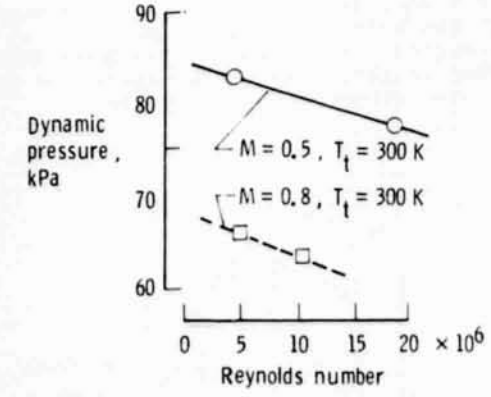

(b) Reynolds number effects.

Figure 12. Cryogenic flutter results and Reynolds number effects.

IV. CONFIGURATIONS

Many new and advanced aircraft configurations and concepts are tested in the TDT, sometimes jointly with the Department of Defense and industry, to understand more fully the often complex aeroelastic behavior of the systems. Some of the studies recently completed are described here.

Body-Freedom Flutter

Body-freedom flutter is a phenomenon that results from the coupling of vehicle rigid body degrees of freedom with the flexible degrees of freedom of the vehicle structure. It has occurred on a modified B-57 in flight (unpublished data) and has been demonstrated in wind-tunnel tests of an oblique wing[11]. Predicted to occur on a forward-swept-wing (FSW) design[12], body-freedom flutter (BFF) was a concern for the X-29A aircraft. A half-scale model (Fig. 13) of an early FSW design was tested[13] in the TDT on a cable and rod mount system that provided the necessary pitch and plunge degrees of freedom for BFF. Of particular interest was the relationship of BFF speed to the static divergence speed of the wing which was designed to divergence criteria. In addition, the model was equipped with a stability augmentation system (SAS) that allowed the comparison of BFF speeds of statically stable and unstable configurations. A hydraulically actuated canard was used to provide the SAS forces.

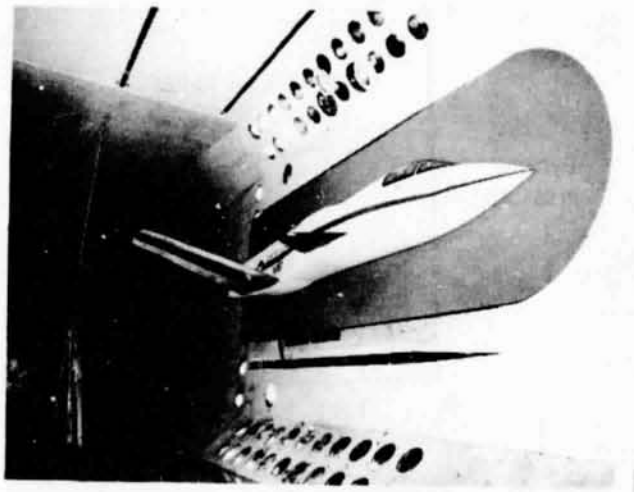

Figure 13. Forward-swept-wing (FSW) model.

Some results of these tests are shown in Fig. 14. A summary of all the test results is shown in Fig 14a. A divergence band was predicted from data that was acquired on the freely flying model at various angles of attack and at dynamic pressures far removed from the instability. (These are some of the reasons that the band is rather large.) The BFF band represents the accumulation of subcritical response predictions and "hard" flutter points for both statically stable and unstable configurations. Little difference was seen in the BFF results of these configurations because the RSS control laws were designed to provide the same flying qualities as the statically stable case. The results in Fig. 14a show that BFF occurred at dynamic pressures approximately 20 to 40 percent lower than divergence. Servo-aero-elastic analysis methods which incorporated doublet-lattice aerodynamics modified by static aeroelastic

test data adequately predicted the BFF instability boundary. A typical analysis/experiment correlation (Fig. 14b) shows that the analysis predicted the BFF fairly well, except in the transonic region where it was somewhat unconservative.

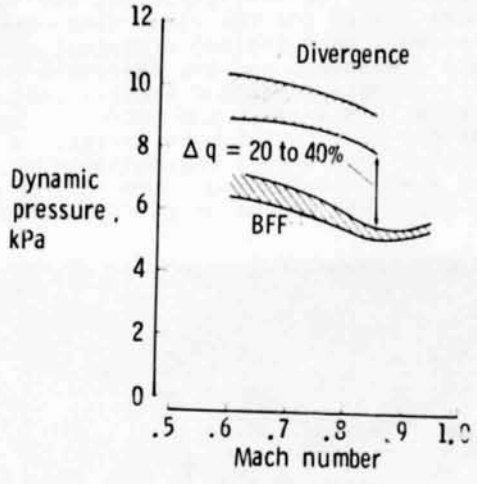

(a) Summary of all test results.

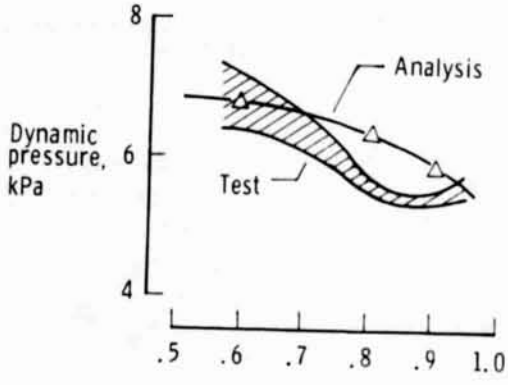

(b) Analysis/test correlation for RSS case.

Figure 14. Results of FSW model test.

Tilt-Rotor Instabilities

The Joint Advanced Vertical Lift (JVX) aircraft design has wing-tip mounted tilting engines driving proprotors that allow operations in both a low-speed helicopter mode and a high-speed airplane mode. A 0.20-scale aeroelastic semi-span model (Fig. 15) of the JVX design was tested[14] in the TDT to determine wing/rotor stability in the airplane mode and to evaluate various design updates and flight parameters. Some of the parameters that were tested include the following: rotor RPM, wing-spar stiffness, rotor-blade stiffness, engine-pylon-to-wing locking (on and off downstop), and coning-hinge-hub stiffness. Flutter conditions were extracted from measured damping data that were acquired using a unique excitation system which incorporated a Freon jet mounted in the wing. Some results of the tests are shown in Fig. 16 for the critical wing-beam (out-of-plane motion) flutter mode. The data at 100 percent rotor speed show that the model with the pylon unlocked from the wing is only slightly less stable than the locked (on downstop) condition. A stiff spar was effective in increasing the flutter speed of the locked-pylon case but did not affect the unlocked-pylon case. A coning hinge hub effectively increased the flutter speed of both pylon cases.

Figure 15. 0.2-scale tilt-rotor model.

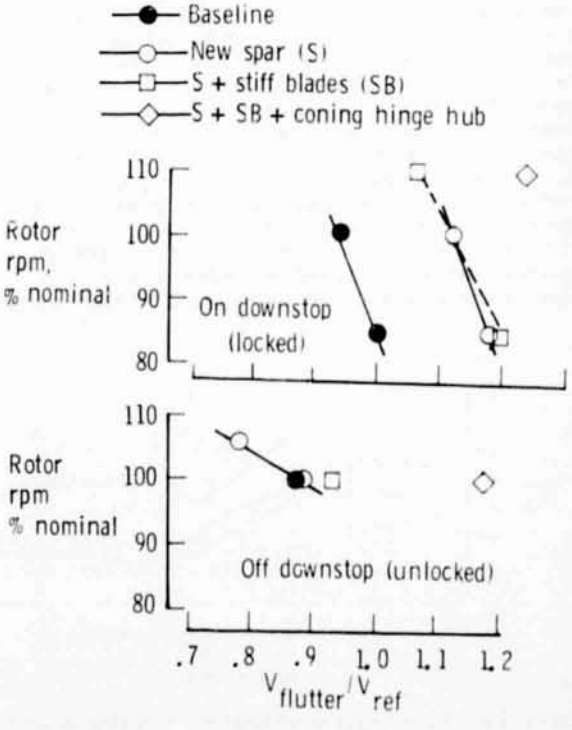

Figure 16. Airplane mode instability boundaries.

Wing-Plus-Winglet Flutter

Winglets are small near-vertical lifting surfaces attached to the tips of wings and have been shown to be effective in increasing the aerodynamic performance of wings[15]. However, the additional mass and aerodynamic forces of the winglet can degrade the flutter performance of the wing. To evaluate the effect on flutter of winglets, several studies were conducted in the TDT.

Figure 17. Winglet on clean wing.

Clean Wing. A 0.154-scale semispan wing model (Fig. 17) of an executive-transport jet aircraft was tested[16]. The wing had a leading-edge sweep angle of 29°, a panel aspect ratio of 3.7, and a supercritical airfoil. The model was tested with three wing tip configurations. They include a normal wing tip, a wing tip with a winglet, and a wing tip that was ballasted to simulate the mass and inertia properties of the winglet. Flutter results for the three configurations were used to separate the aerodynamic and mass effects. These flutter boundaries are presented in Fig. 18 and show that the winglet and ballasted-tip configurations had lower transonic flutter speeds than the normal tip configuration. At 0.8 Mach number the flutter speed was reduced approximately five percent due to mass alone and seven percent due to the winglet addition. Therefore, the aerodynamic effect caused a reduction of approximately two percent in flutter speed.

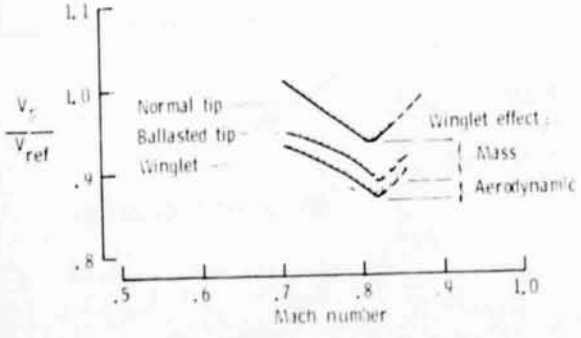

Figure 18. Winglet effects on wing-alone flutter speed.

Wing With Single Engine. A 0.10-scale semispan wing model[17] of a large twin-engine transport aircraft also was flutter tested with and without a winglet. A picture of the model mounted in the TDT is shown in Fig. 19. The wing had a quarter-chord sweep angle of 31°, a panel aspect ratio of 3.5, and an advanced airfoil. Three wing tip configurations similar to those tested for the clean wing were studied. They include a nominal one, one with a winglet, and one ballasted to simulate winglet mass and inertia characteristics. Typically, the three configurations were tested with variations in winglet cant angle, engine pylon stiffness and wing fuel loading. Some of the results of the tests are shown in Fig. 20 for the

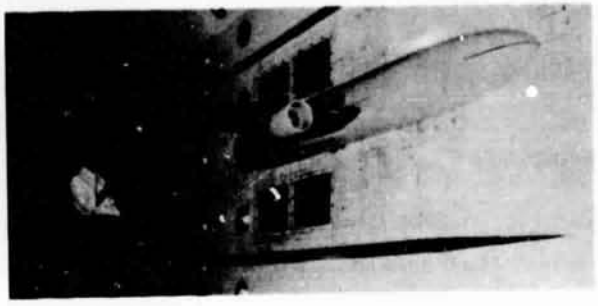

Figure 19. Winglet on wing-with-engine configuration.

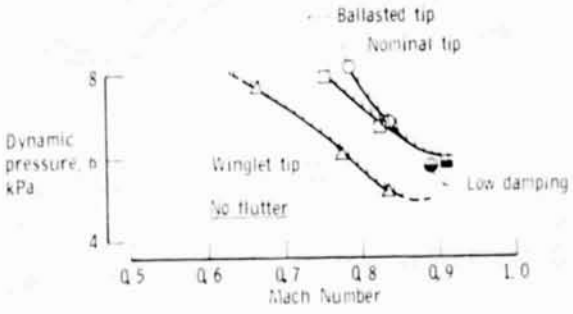

Figure 20. Winglet effects on wing-with-engine flutter boundary.

empty wing (no fuel) case. For this model the addition of the winglet lowered the flutter boundary in the transonic region. However, the reduction in flutter dynamic pressure (nearly 20 percent near the dip) was predominately due to aerodynamic effects. Other results indicated that changing the cant angle from 20° to 0° had little effect on the flutter speed near the transonic dip but slightly reduced the speed at lo r subsonic Mach numbers.

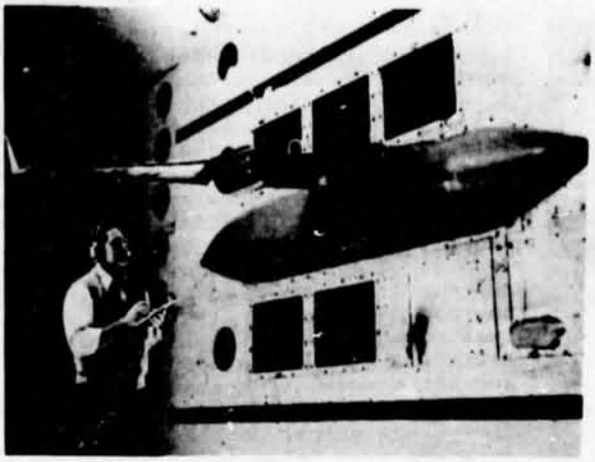

Figure 21. Winglet on wing with two engines.

Wing With Two Engines. A 0.08-scale semispan wing model of an advanced large transport aircraft with four engines also was tested[3]. A picture of the model in the TDT is shown in Fig. 21. Model wingtip configurations that were tested include the following: one with a basic winglet, one with a lightweight winglet, and one ballasted with a boom to simulate the winglet mass and inertia properties of the basic winglet. Test results indicate that the winglet aerodynamics slightly increased (7 percent) the flutter dynamic pressure of the ballasted configuration. Flutter analyses of the configurations were conducted for correlation with the experimental results. A typical experiment/analysis correlation of transonic flutter data is shown in Fig. 22. The "no flutter" point is the maximum velocity at which the model was tested at Mach numbers higher than 0.8. The analysis, which used doublet-lattice aerodynamics that was corrected by a scalar (based on experimental steady state data), agreed well at the transonic dip but was somewhat conservative at lower Mach numbers. The flutter mode in all cases was a coupling of the outer-wing-bending and wing-torsion modes and was strongly influenced by the presence of the winglet.

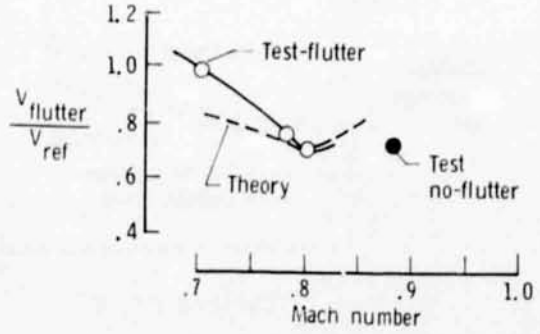

Figure 22. Winglet on wing-with-engines flutter boundary

Airfoil Shape Effects

The supercritical wing[18] was designed to reduce the normal shock effects on lift and drag at transonic Mach numbers. An experimental study[19] in the TDT showed that a wing with a supercritical airfoil shape had lower flutter speeds than a similar wing with a conventional airfoil shape. Since those tests, additional studies have been conducted on models in the TDT.

Wings on PAPA. Two unswept wings with a panel aspect ratio of three were tested[9] using the PAPA. One had a NACA 64A010 conventional airfoil shape and the other had a symmetric (uncambered) supercritical airfoil shape. Both airfoils were ten percent thick. The resulting flutter boundaries and flutter frequencies are presented in Fig. 23. The results are similar to those found in Ref. 19 in that the wing with the supercritical airfoil had a flutter boundary lower than that of the conventional wing. At the bottom of the transonic dip, the flutter dynamic pressure of the supercritical wing was approximately 11 percent lower than that of the conventional wing. The flutter frequencies were almost identical for the two wings, except at the highest Mach number point where the supercritical wing frequency was higher than for the conventional wing.

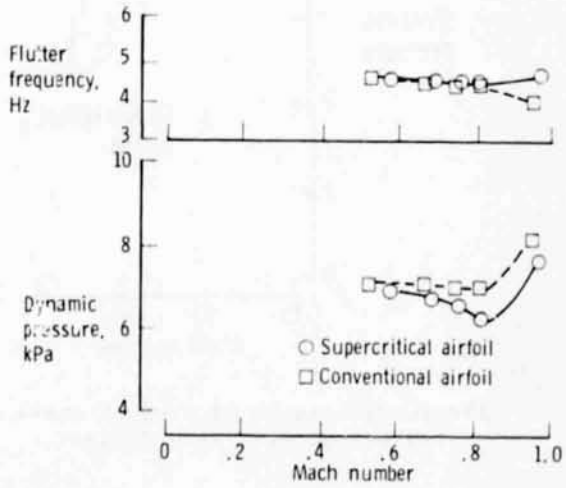

Figure 23. Effect of airfoil shape on flutter of models on PAPA.

Wing With Engines. The effect of airfoil shape on flutter was investigated[20] on another model in the TDT. This was a 0.083-scale semispan model (Fig. 24) of a large transport-type wing with two pylon-mounted engines. The wing had a panel aspect ratio of four. The model was constructed using a wing spar with interchangeable airfoil pods attached. The wing stiffness was isolated in the wing spar; the wing mass properties were isolated in the airfoil pods. The two airfoil shapes included a conventional airfoil and an advanced supercritical airfoil. The wing was

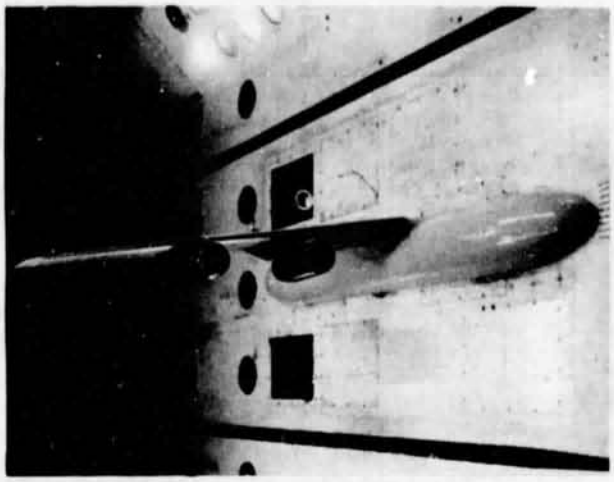

Figure 24. Supercritical airfoil on wing-with-engines model.

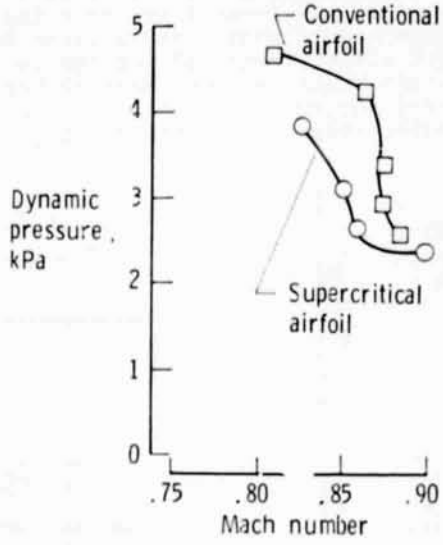

Figure 25. Effect of airfoil shape on flutter of wing with engines.

mounted to a fuselage half body that was cantilevered from the sidewall. Results of the tests are shown in Fig. 25. Similar to previous tests, the transonic flutter boundary of the supercritical airfoil configuration was lower than that of the conventional airfoil. The onset of the transonic dip occurred at a slightly lower Mach number for the supercritical airfoil.

Curvature Effect on Flutter

Some new missile configurations require curved lifting surfaces that can be wrapped around the body for storage and then unwrapped for use in flight. In order to determine the effect on flutter of wing spanwise curvature, a series of models as shown in Fig. 26 was tested[3] in the TDT. The models were constructed of aluminum plate and foam and had values of curvature (inverse of radius r) ranging from zero to 3.44 per meter (1.05 per foot). The panel aspect ratio of each wing was 1.5. Results of the tests and comparative analyses are shown in Fig. 27 for a typical Mach number of 0.7. The results show that the flutter dynamic pressure increased as the curvature increased. This results from the change in torsion mode shape--that is, as the curvature increases, the motion in the fore-and-aft direction becomes dominant, displacing the motion perpendicular to the flow. Analytical predictions (Fig. 27) obtained from using kernel-function and doublet-lattice aerodynamics bracket the experimental results with the doublet-lattice results being more conservative than the experimental results.

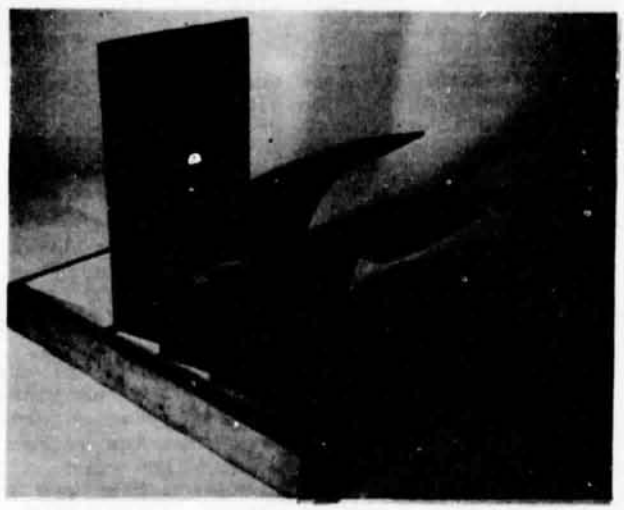

Figure 26. Spanwise-curved wing models.

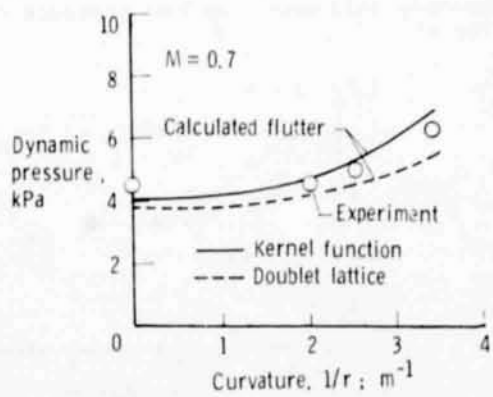

Figure 27. Effect of spanwise curvature on transonic flutter dynamic pressure.

DAST Wing Instability

The DAST (Drones for Aerodynamic and Structural Testing) program[21] has been underway at NASA for a number of years. In this program research wings were flight tested on a drone to measure aerodynamic pressure distributions and aeroelastic performance. One of the wings being prepared for flight is an aft-swept design with a leading-edge sweep of 29°, a panel aspect ratio of 5.1, and a supercritical airfoil shape. The wing has active controls for flutter suppression, gust load alleviation, maneuver load control and stability augmentation. Instrumentation to measure steady and unsteady aerodynmic loads is also installed. This wing (Fig. 28) was tested in the TDT to acquire wind-tunnel data for comparison with analytical results and future flight test data.

Figure 28. Semi-span DAST flight research wing.

Results of the tunnel test[22] are shown in Fig. 29. An unexpected flutter instability in the transonic region was encountered at nearly constant Mach number (0.9) extending from low dynamic pressure to near the dynamic pressure limit of the tunnel. The motion was predominantly wing bending which varied in frequency from 8.6 Hz (wind-off wing first bending frequency was 8.3 Hz) at the lowest dynamic pressure to 13 Hz at the highest dynamic pressure. The predicted flutter frequency using linear theory is 24 Hz at 0.8 Mach number. Flutter points were measured in both Freon-12 and air test mediums and with and without transition strips. Results of all these test conditions were similar. It is speculated that the instability is a "shock-induced oscillation," or one driven by shock motion. Pressure data acquired during the test are being studied to determine the location and movement of the shock during the oscillations. Additional testing of the wing is planned to determine the effectiveness of the flutter suppression system to control the instability. Furthermore, the increased capability of the TDT will be used to extend the instability boundary to higher dynamic pressures toward the predicted flutter boundary (Fig. 29).

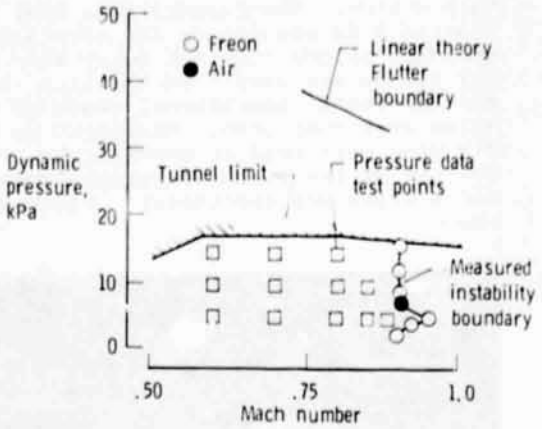

Figure 29. DAST transonic instability boundary.

Passive Flutter Suppression

Stores added to a wing often degrade the flutter performance of the wing because the added pitch inertia of the stores tends to lower the frequency of the wing torsion mode. A "decoupler pylon" concept[23] was developed to uncouple the inertia of a store from that of the wing. The pylon attaches a store to the wing through a simple system of pinned linkages, springs, and dampers. Initial research results were reported at the first aeroelasticity symposium in 1981. Since that time, an advanced pylon[24] has been designed and tested on the F-16 airplane both in the wind tunnel (Fig. 30) and in flight (Fig. 31). In Fig. 32, typical wing-tip accelerometer time histories[3] are presented for the two pylon configurations flown at 0.9

Figure 30. Model with decoupler pylons.

Mach number. The results show that the flutter mode present on the airplane with standard pylons does not occur when decoupler pylons are used. In addition to the flutter tests, operational tests of the pylon were conducted. Maneuvers up to four g's were performed to demonstrate the capability of the store alignment mechanism, and a store was successfully ejected from the pylon.

Figure 31. Flight demonstration of decoupler pylons.

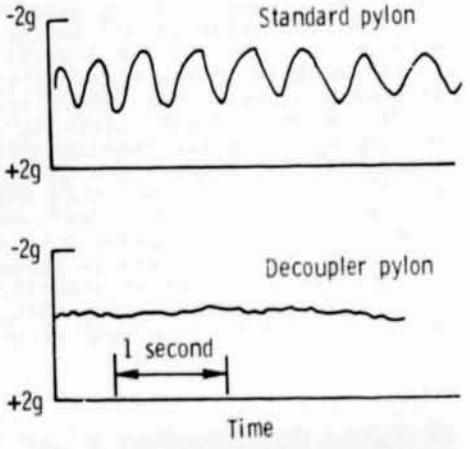

Figure 32. Wing tip accelerations for standard and decoupler pylons.

V. CONCLUDING REMARKS

Some results of recently completed experimental studies in aeroelasticity performed by NASA Langley Research Center, primarily at the TDT and sometimes in cooperation with the Department of Defense and industry, have been presented. The studies included the investigation of the impact of innovative aerodynamic and structural changes on the flutter stability of basic configurations as well as the stability of new configurations. In addition, new methods of testing for aeroelastic phenomena were highlighted. NASA will continue to conduct research in aeroelasticity through the coming years to expand the data base of information, to try to understand more fully the mechanisms involved, and to exploit aeroelasticity to advance the state of the art in aerospace vehicle design.

VI. REFERENCES

1. Gardner, James E.: Loads and Aeroelasticity Division Research and Technology Accomplishments for FY 1982 and Plans for FY 1983. NASA TM 84594, January 1983.

2. Gardner, James E.; and Dixon, S. C.: Loads and Aeroelasticity Division Research and Technology Accomplishments for FY 1983 and Plans for FY 1984. NASA TM 85740, January 1984.

3. Gardner, James E.; and Dixon, S. C.: Loads and Aeroelasticity Division Research and Technology Accomplishments for FY 1984 and Plans for FY 1985. NASA TM 86356, January 1985.

4. Reed, W. H., III: Aeroelasticity Matters--Some Reflections on Two Decades of Testing in the NASA Langley Transonic Dynamics Tunnel. Proceedings of the First International Symposium on Aeroelasticity, Nuremberg, Germany, October 5-7, 1981. (Also available as NASA TM 83210, September 1981.)

5. Sandford, Maynard C.; Ricketts, Rodney H.; and Hess, Robert W.: Recent Studies on Transonic Unsteady Pressure Measurements at the NASA Langley Research Center. Proceedings of the Second International Symposium on Aeroelasticity and Structural Dynamics, Aachen, Germany, April 1-3, 1985.

6. Cole, Patricia H.: Wind Tunnel Real-Time Data Acquisition System. NASA TM 80081, April 1979.

7. Ray, Edward J.: A Review of Reynolds Number Studies Conducted in the Langley 0.3-m Transonic Cryogenic Tunnel. Proceedings of the AIAA/ASME 3rd Joint Thermophysics, Fluids, Plasma and Heat Transfer Conference, St. Louis, Missouri, June 7-11, 1982. AIAA Paper No. 82-0941, 1982.

8. Ruhlin, Charles L.; Watson, Judith J.; Ricketts, Rodney H.; and Doggett, Robert V., Jr.: Evaluation of Four Subcritical Response Methods for On-Line Prediction of Flutter Onset in Wind Tunnel Tests. AIAA Journal of Aircraft, Vol. 20, No. 10, October 1983.

9. Farmer, Moses G.: A Two-Degree-of-Freedom Flutter Mount System with Low Damping for Testing Rigid Wings at Different Angles of Attack. NASA TM 83302, April 1982.

10. Cole, Stanley R.: Exploratory Flutter Test in a Cryogenic Wind Tunnel. Proceedings of the AIAA/ASME/ASCE/AHS 26th Struc-

tures, Structural Dynamics and Materials Conference, Orlando, Florida, April 15-17, 1985. AIAA Paper No. 85-0736-CP, 1985.

11. Jones, R. T.: Aeroelastic Stability and Control of an Oblique Wing--Wind Tunnel Experiments. Journal of Aircraft, Vol. 13, No. 10, October 1976.

12. Miller, Gerald D.; Wykes, John H.; and Brosnan, Michael J.: Rigid Body-Structural Mode Coupling on a Forward Swept Wing Aircraft. Proceedings of the AIAA/ASME/ASCE/AHS 23rd Structures, Structural Dynamics and Materials Conference, New Orleans, Louisiana, May 10-12, 1982. AIAA Paper No. 82-0683, 1982.

13. Chipman, Richard; Rauch, Frank; Rimer, Melvyn; Muniz, Benigno; and Ricketts, Rodney H.: Transonic Test of a Forward-Swept-Wing Configuration Exhibiting Body-Freedom Flutter. Proceedings of the AIAA/ASME/ASCE/AHS 26th Structures, Structural Dynamics and Materials Conference, Orlando, Florida, April 15-17, 1985. AIAA Paper No. 85-0689-CP, 1985.

14. Mantay, Wayne R.; Yeager, William T., Jr.; Hamouda, M-Nabil H.; Cramer, Maj. Robert G., Jr.; and Langston, Chester W.: Aeroelastic Model Helicopter Rotor Testing in the Langley TDT. Proceedings of the AHS Specialists' Meeting on Helicopter Test Methodology, Williamsburg, Virginia, October 29 - November 1, 1984.

15. Whitcomb, Richard T: Design Approach and Selected Wind-Tunnel Results at High Subsonic Speeds for Wing-Tip Mounted Winglets. NASA TN D-8260, 1976.

16. Ruhlin, C. L.; Rauch, F. J.; and Waters, C.: Transonic Flutter Model Study of a Supercritical Wing and Winglet. Journal of Aircraft, Vol. 20, No. 8, August 1983.

17. Bhatia, Kumar G.; Nagaraja, K. S.; and Ruhlin, Charles L.: Winglet Effects of the Flutter of Twin-Engine-Transport-Type Wing. Proceedings of the AIAA/ASME/ASCE/AHS 25th Structures, Structural Dynamics and Materials Conference, Palm Springs, California, May 14-16, 1984. AIAA Paper No. 84-0905-CP, May 1984.

18. Whitcomb, Richard T: Review of NASA Supercritical Airfoils. ICAS Paper No. 74-10, August 1974.

19. Farmer, Moses G.; Hanson, Perry W.; and Wynne, Eleanor C.: Comparison of Supercritical and Conventional Wing Flutter Characteristics. Proceedings of the AIAA/ASME/SAE 17th Structures, Structural Dynamics and Materials Conference, King of Prussia, Pennsylvania, May 5-7, 1976. (Also available as NASA TM X-72837, 1976.)

20. Grosser, W. F.; Britt, R. T.; Childs, C. B.; Crooks, O. J.; and Cazier, F. W., Jr.: Flutter and Steady/Unsteady Aerodynamic Characteristics of Supercritical and Conventional Transport Wings. AGARD-R-703, January 1983.

21. Murrow, H. N.; and Eckstrom, C. V.: Drones for Aerodynamic and Structural Testing (DAST) - A Status Report. Journal of Aircraft, Vol. 16, No. 8, August 1979.

22. Seidel, David A.; Sandford, Maynard M.; and Eckstrom, Clinton V.: Measured Unsteady Transonic Aerodynamic Characteristics of an Elastic Supercritical Wing with an Oscillating Control Surface. Proceedings of the AIAA/ASME/ASCE/AHS 26th Structures, Structural Dynamics and Materials Conference, Orlando, Florida, April 15-17, 1985. AIAA Paper No. 85-0598-CP, 1985.

23. Reed, W. H., III; Foughner, Jerome T., Jr.; and Runyan, Harry L., Jr.: Decoupler Pylon--A Simple, Effective Wing/Store Flutter Suppressor. Journal of Aircraft, Vol. 17, No. 3, March 1980.

24. Peloubet, R. P., Jr.; Haller, R. L.; and McQuien, L. J.: Feasibility Study and Conceptual Design for Application of the NASA Decoupler Pylon to the F-16. NASA CR 165834, May 1982.

1. Report No.	2. Government Accession No.	3. Recipient's Catalog No.
NASA TM-86436		

4. Title and Subtitle	5. Report Date
Selected Topics in Experimental Aeroelasticity at the NASA Langley Research Center	April 1985
	6. Performing Organization Code 505-33-43-07

7 Author(s)	8. Performing Organization Report No.
Rodney H. Ricketts	
	10 Work Unit No.

9 Performing Organization Name and Address	11 Contract or Grant No
NASA Langley Research Center Hampton, VA 23665	
	13 Type of Report and Period Covered
12 Sponsoring Agency Name and Address	Technical Memorandum
National Aeronautics and Space Administration Washington, DC 20546	14 Sponsoring Agency Code

15 Supplementary Notes

This paper (paper no. 85-70) was presented at the Second International Symposium on Aeroelasticity and Structural Dynamics, April 1-3, 1985, Aachen, Germany.

16 Abstract

The National Aeronautics and Space Administration (NASA) conducts research in aeroelasticity to develop new technologies for aerospace-vehicle applications, to study innovative configuration changes for improved flight performance, and to develop new methods of testing for aeroelastic instabilities. This paper presents the results of selected studies that have been conducted by the NASA Langley Research Center in the last three years. The topics presented focus primarily on the ever-important transonic flight regime and include the following: body-freedom flutter of a forward-swept-wing configuration with and without relaxed static stability; instabilities associated with a new tilt-rotor vehicle; effects of winglets, supercritical airfoils, and spanwise curvature on wing flutter; wind-tunnel investigation of a "flutter-like" oscillation on a high-aspect-ratio flight research wing; results of wind-tunnel demonstration of the NASA decoupler pylon concept for passive suppression of wing/store flutter; and, new flutter testing methods which include testing at cryogenic temperatures for full scale Reynolds number simulation, subcritical response techniques for predicting onset of flutter, and a two-degree-of-freedom mount system for testing side-wall-mounted models.

17. Key Words (Suggested by Author(s))	18. Distribution Statement
Aeroelasticity Wind-tunnel tests Flutter Transonic speeds	Unclassified-Unlimited Subject Category 39

19. Security Classif. (of this report)	20. Security Classif. (of this page)	21. No. of Pages	22. Price
Unclassified	Unclassified	14	A02

For sale by the National Technical Information Service, Springfield, Virginia 22161